Parameter analysis of a pair of Bragg gratings with overlapping spectra for power measurement of small deformations

M. FAJKUS[a,*], M. NOVAK[b], J. NEDOMA[b], E. HRUBESOVA[a], P. MEC[c], R. MARTINEK[d]
[a]*Department of Department of Geotechnics and Underground Engineering, Faculty of Civil Engineering, VSB - Technical University of Ostrava, 17. listopadu 15/2172, 708 33 Ostrava, Czech Republic*
[b]*Department of Telecommunications, Faculty of Electrical Engineering and Computer Science, VSB - Technical University of Ostrava, 17. listopadu 15/2172, 708 33 Ostrava, Czech Republic*
[c]*Department of Building Materials and Diagnostics of Structures, Faculty of Civil Engineering, VSB - Technical University of Ostrava, 17. listopadu 15/2172, 708 33 Ostrava, Czech Republic*
[d]*Department of Cybernetics and Biomedical Engineering, Faculty of Electrical Engineering and Computer Science, VSB - Technical University of Ostrava, 17. listopadu 15/2172, 708 33 Ostrava, Czech Republic*

Bragg gratings belong to a group of single-point fibre optic sensors that can be simply multiplexed to achieve quasi-distributed sensing. As for single-point measurement, conversion of a spectral shift to a reflected power change allows replacing a complex and costly evaluation unit with a low-cost optical performance monitoring system. This article deals with the design of parameters of a pair of Bragg gratings with overlapping reflection spectra for transforming a spectral shift into a power change. The parameter analysis of Bragg gratings was performed in the OptiSystem SW environment to achieve a large measurement range with a linear response to the measurand. The measurement concept designed is immune to temperature changes. The functionality of the concept was experimentally verified during the measurement of deformation.

(Received July 26, 2018; accepted April 8, 2019)

Keywords: Fibre Bragg grating, Sensor, OptiSystem, Power measurement, Passive detection scheme

1. Introduction

Bragg gratings are the most widely used fibre-optic sensors; their principle is based on the change in the spectral properties of the reflected light by the action of the measurand. Costly optical spectrum analysers are used to evaluate up to tens of FBG sensors. Cheaper options can be used for single-point measurements. These are based, for example, on conversion of a spectral shift to a power change.

The authors of the publications [1-2] describe passive detection systems that can sense physical quantities, typically deformation or temperature. Both systems published use division of the light reflected from the FBG into two branches. The wave-dependent filter in one (measuring) branch whose transmittance is dependent on the spectral position of the transmitted light modulates the output power according to the change in the wavelength of the light. The second (reference) branch serves for detecting fluctuations in optical power due to fluctuations in power of a broadband source, etc. These optical signals are then converted into an electrical area. The resulting power signal corresponding to the load on the Bragg grating is then determined by the ratio of both signals, i.e. PM/PR. The resolution of deformations achieved in the dynamic processes was 7.8 μstrain. A similar solution is shown by the authors in the article [3], where the wave-dependent filter is replaced, in one branch, by a Bragg grating that performs the same function. The minimum detectable boundary is 5.2 μstrain for the static load system and 1.2 μstrain for the dynamic load system. Other detection systems with Bragg gratings [4-6] use a similar principle, with the exception that a wave-dependent coupler is integrated into the system. A typical resolution of such systems oscillates about 3 μstrain for a static load while it is less than 1 μstrain for dynamic resolutions. Wave-dependent filters showed a constant change in the bonding ratio of 0.4 dB/nm in the range from 1520 to 1560 nm. The articles [7-8] describe different approaches to passive sonsoric systems with two chirped Bragg gratings, one of which is a sensor one and the other one performs the function of a filter. Due to the use of chirped gratings with a wider reflection spectrum, it is possible to increase the measurement range up to the value of 1800 μstrain.

The second group consists of active detection schemes that use more complex principles such as scanning or modulation of light and also offer higher resolution.

The first approach described in the article [9] uses processing of light reflected from the Bragg grating in a Michelson interferometer, where one branch is stretched in the range of 0 to 10 cm on a piezoelectric transducer. The signal from the interferometer is processed by the Fourier Transform, the output of which is the optical spectrum of the light processed from the FBG. Using this technique, resolution of 15 pm was achieved in the spectral region. The modified version [10] uses scanning of a considerably

shorter length, 1.2 mm, thereby increasing the resolution to 5 pm. Another approach is based on an acousto-optical filter that uses modulation of optical light power by acoustic waves. The wavelength of the reflected light is determined by the maximum power at the photodetector that is dependent on the frequency of the sound waves. The range of wobbled sound waves must be pre-calibrated to a certain optical spectrum [11]. Multi-point evaluation using an acousto-optical tuning filter is discussed in the article [12], or in the article [13], where a deformation coefficient of 96.6 Hz/μstrain was achieved.

This article deals with a power detection system using a pair of Bragg gratings with overlapping spectra. The objective of this article is to find suitable parameters for a pair of Bragg gratings to achieve the best linearity of the conversion characteristic and the largest measurement range.

2. Methods

Photosensitivity of the germanium-doped optical fibre was discovered in 1978 by K. O. Hill, when the attenuation increased after a long exposure of the optical fibre at a wavelength of 488 nm [14]. Photosensitivity is a feature that allows change in the magnitude of the refractive index in the photosensitive optical fibre core by UV radiation of a specific wavelength and intensity, thereby developing the structure of the Bragg grating.

Fig. 1 shows the structure of a uniform Bragg grating formed by a periodic change in the refractive index of the optical fibre core.

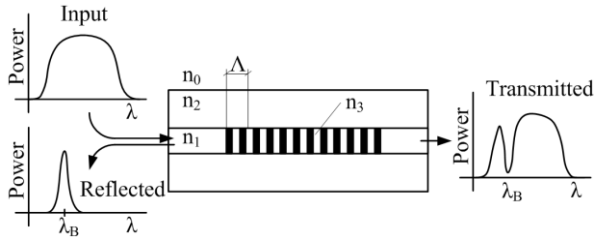

Fig. 1. Fibre Bragg grating structure

when wide-spectrum light passes through the optical fibre, the Bragg grating structure selectively reflects a specific wavelength called the Bragg wavelength and is given by the following relationship:

$$\lambda_B = 2n_{eff}\Lambda, \tag{1}$$

where n_{eff} is the effective refractive index determined by the FBG structure and Λ is the refractive index change period [15].

Bragg gratings form an alternative approach to conventional electrical sensors of a range of variables such as temperature, deformation, pressure, acceleration, shift, etc. [16]. The external effect of temperature T or deformation ε on the Bragg grating causes the Bragg wavelength to be shifted according to the following relation:

$$\frac{\Delta\lambda}{\lambda_0} = k\varepsilon + (\alpha_\Lambda + \alpha_n)\Delta T, \tag{2}$$

where k is the deformation coefficient, α_Λ is the coefficient of thermal expansion, and α_n is the thermo-optic coefficient. The previous relation defines the deformation and temperature sensitivity of the Bragg grating with respect to the spectral position of the Bragg wavelength. This relative sensitivity is often expressed using the standard deformation coefficient at constant temperature:

$$\frac{1}{\lambda_B}\frac{\Delta\lambda_B}{\Delta\varepsilon} = 0{,}78.10^{-6} \quad \mu strain^{-1} \tag{3}$$

and a standardized temperature coefficient at constant deformation:

$$\frac{1}{\lambda_B}\frac{\Delta\lambda_B}{\Delta T} = 6{,}678.10^{-6} \quad ^\circ \quad C^{-1}. \tag{4}$$

Bragg gratings are single-point sensors which can easily be multiplexed using wave or time multiplex to achieve multipoint measurement [17-19].

2.1. A detection scheme with a pair of Bragg gratings

The simplest approach to evaluating one or more Bragg sensors is to use an optical spectral analyser. The condition is that each sensor is to be set to a different Bragg wavelength. This approach allows evaluation of tens of sensors at the same time. The disadvantage is the high purchase price of the optical spectrum analyser or the evaluation unit. When using a fibre-optic grating sensor for single-point deformation measurement, it is possible to use a simpler and cheaper approach. The most economically advantageous approach is based on conversion of a spectral shift of the Bragg wavelength to a change in power detected by the photodetector.

The detection scheme uses wide-spectrum light, which is led, via a circulator, to a pair of Bragg gratings with partially overlapping reflection spectra. The reflected light is fed to a photodetector (Pm), digitized by an analog/digital converter (A/D), and further processed on a computer (PC). The arrangement of the system described is shown in Fig. 2.

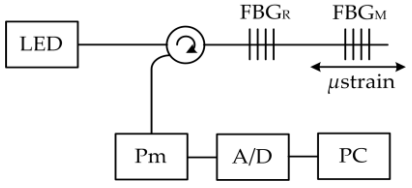

Fig. 2. The principle of the detection scheme with a pair of Bragg gratings

The sensing part of the measuring system consists of a Bragg measuring sensor FBG_M and a reference Bragg sensor FBG_R. The measuring sensor is attached to the structure measured so that the deformations from the structure were transmitted to the Bragg grating. The reference sensor is installed based on deformation insensitivity. The advantage of this approach is automatic temperature impact compensation because both gratings are affected by the temperature equally.

The light reflected from the Bragg gratings (FBG_M and FBG_R) is characterized by two partially overlapping spectra in the unloaded state as shown in Fig. 3a. The total reflected power is determined by the area under both spectra. By the action of for example deformation, the spectrum of the FBG_M measuring grating is shifted, the area, and hence the total reflected power that is recorded by the photodetector (Fig. 3b), is increased. This assures the conversion of the spectral shift of the measurement Bragg grating to power change.

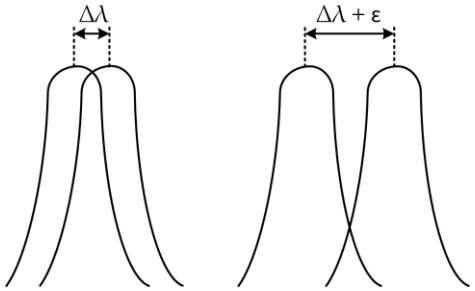

Fig. 3. The reflection spectrum of a pair of Bragg gratings (a) in the unloaded state; (b) in the loaded state (b)

The general dependence of power change on the spectral shift of the measurement Bragg grating is shown in Fig. 4. The ideal conversion characteristic is formed in the working area of the linear part that is suitable for measurement. The magnitude of the measurement range, i.e. the interval of deformations in the linear part of the working conversion characteristic, is also important.

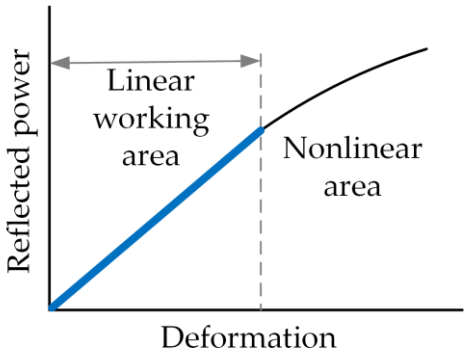

Fig. 4. The conversion characteristic of the power detection scheme with a pair of Bragg gratings with overlapping spectra

The linear part of the conversion characteristic and the sufficient range of the measurement range are the conditions for using power measurement. Both of these requirements depend on the shape of the reflection spectrum of the pair of gratings in the unloaded state. This is the distance between the overlapping neighbouring spectra, their width and the reflectivity of the Bragg gratings, i.e. the edge steepness of the spectra.

3. Simulation

The determination of the appropriate parameters of the pair of Bragg gratings for power measurement was conducted in the OptiSystem simulation environment. In order to connect two Bragg gratings in series, a block of a Bragg sensor was created, comprising two input ports and two output ports (Fig. 5a). The block was also created for the purpose of adjusting the size of the deformations acting on the Bragg grating measured. The schematic diagram of the entire connection is shown in Fig. 5b.

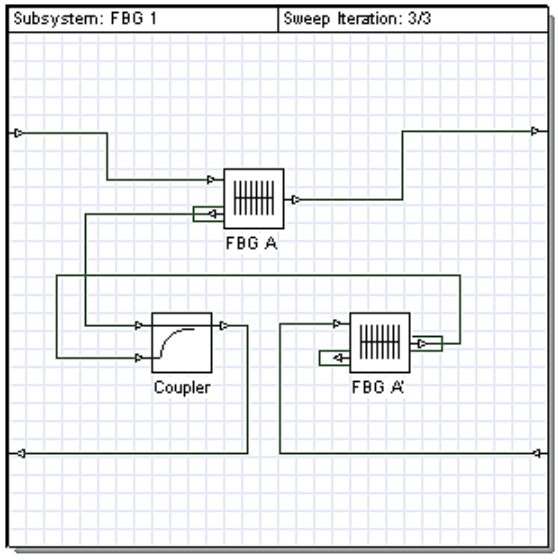

(a)

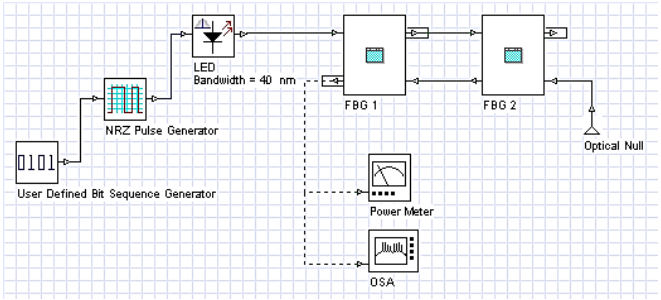

(b)

Fig. 5. The block of a Bragg sensor a); the schematic diagram of the connection. (b)

The simulations were performed for a deformation effect from 0 to 300 μstrain. Fig. 6 shows the dependence

of the reflected power on the applied strain for Bragg gratings with a spectral width of 1 nm and reflectivity of 95% for various distances between neighbouring Bragg wavelengths. At a small distance between the spectra, there is a slow increase in power, while, at a large distance where the spectra overlap only partially, the measurement range is reduced. The figure shows that the optimum distance between the spectra is roughly half the width of the spectrum (the yellow and orange curve).

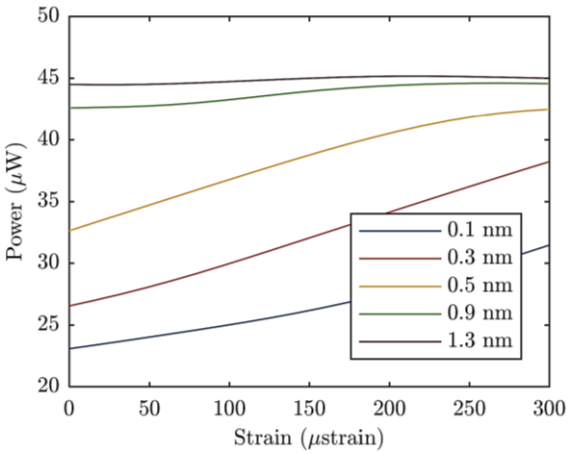

Fig. 6. Reflected power dependence on deformation of a pair of Bragg gratings with reflectivity of 95%, spectral width 1 nm for a different spectral distance between FBGs

An important parameter of the passive detection scheme is the linearity of the conversion characteristic that affects the accuracy of the deformation measurement. Another important parameter of the detection scheme is the deformation measurement range. Figs. 7a-7c show the power measurement ranges for various spectral widths, the distance between the spectra and the reflectivity of the Bragg gratings. Each point is represented by one configuration. In total, simulations for 84 configurations were performed.

Ten configurations were selected from the aforementioned simulations for which the highest power measurement range was achieved with the greatest possible linearity. The parameters of the Bragg gratings of the ten selected configurations are summarized in Table 1. The power measurement ranges vary from 9 to 12 μW. The linearity was determined by the parameter of reliability of the linear approximation and it is higher than 98% with selected configurations. The conversion characteristics of the selected configurations are shown in Fig. 8. Eight out of ten configurations show a linear conversion characteristic in the entire deformation measurement range from 0 to 300 μstrain.

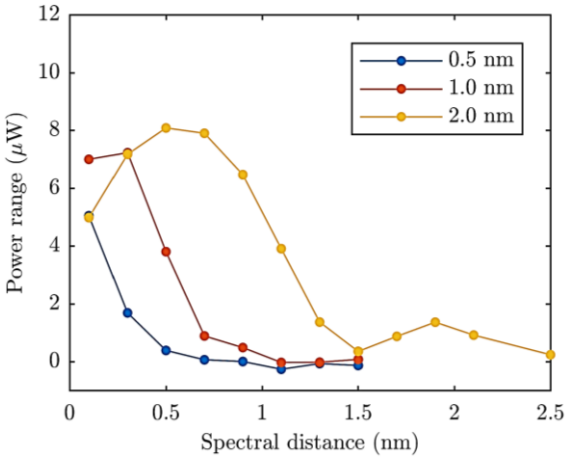

(a)

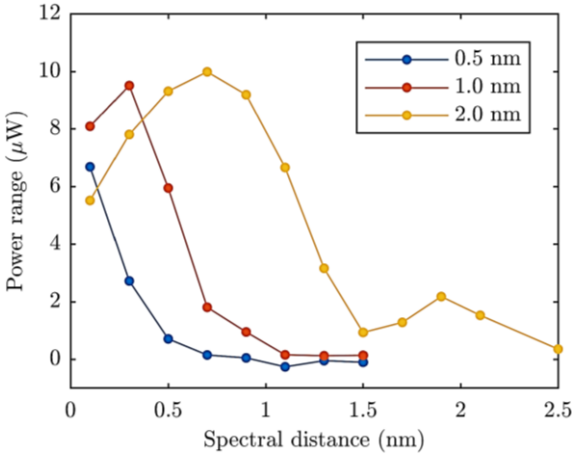

(b)

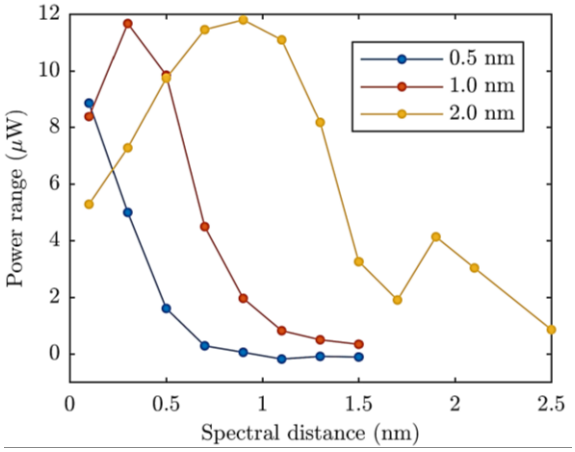

(c)

Fig. 7. Reflected power range dependence on spectral distance between FBGs for a different spectral width of FBG with (a) reflectivity of 75 %; (b) reflectivity of 85 %; (c) reflectivity of 95 %

Table 1. The measurement power range and reliability for the most suitable variants of the pair of Bragg gratings

ID	#1	#2	#3	#4	#5	#6	#7	#8	#9	#10
Shift (nm)	0,3	0,5	0,5	0,7	0,9	1,1	0,3	0,5	0,7	0,9
FWHM (nm)	1	1	2	2	2	2	1	2	2	2
Reflectivity (-)	95	95	95	95	95	95	85	85	85	85
Power range (μW)	11.669	9.847	9.741	11.453	11.797	11.094	9.509	9,.312	9.986	9.190
Sensitivity (mW/strain)	38.896	32.822	32.470	38.177	39.323	36.980	31.696	31.039	33.287	30.634
Reliability (-)	0.999	0.983	0.996	1.000	1.000	0.999	0.999	0.999	1.000	0.998

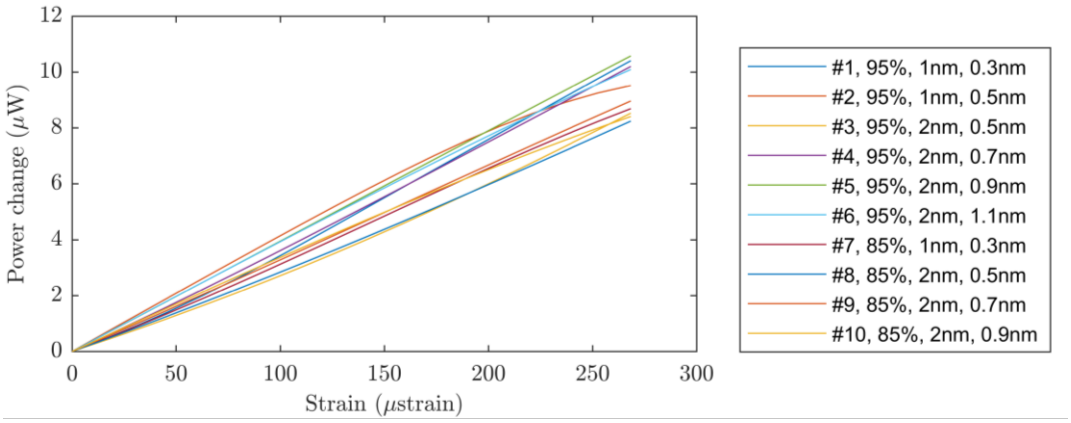

Fig. 8. Dependence of the power change on the acting deformation for the most suitable variant of the pair of Bragg gratings

From this analysis, a suitable configuration of the pair of Bragg gratings can be selected to measure small deformations in the range from 0 to 300 μstrain. This deformation range with respect to the relation (3) for the wavelength around 1550 nm corresponds to the change in the Bragg wavelength of the measurement grating in the range from 0 to about 272 pm. The above-mentioned power measurement can be performed to measure any quantity within the range that causes changes in Bragg wavelengths up to approximately 280 pm.

To achieve larger measurement ranges, it is necessary to use gratings with significantly wider reflection spectra. The following simulations were performed for a deformation effect in an increased range from 0 to 2,000 μstrain. Configuration parameters with the largest measurement range are shown in Table 2. The conversion characteristics are then shown in Fig. 9.

Table 2. The most suitable variant of the pair of Bragg gratings for the measurement of large deformations from 0 to 2000 μstrain

ID	Shift (nm)	FWHM (nm)	R (%)	Range (μstrain)
#1	0.3	1	95	400
#3	0.5	2	95	850
#5	0.9	2	95	550
#7	0.3	1	85	350
#8	0.5	2	85	700

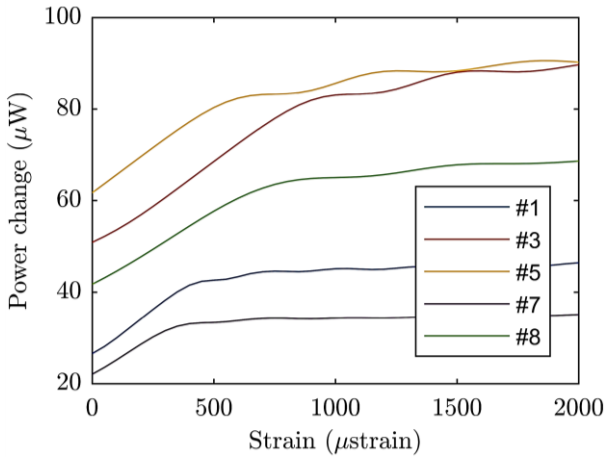

Fig. 9. Results for measurement of larger deformations

The aforementioned conversion characteristics help in selecting the parameters of the pair of Bragg gratings for implementing the power measurement. The results show that the higher the spectral width, the greater the measurement range. On the other hand, the linearity in the working area deteriorates.

4. Experimental setup

The previous simulations showed suitable configurations for the detection scheme with a pair of Bragg gratings with overlapping spectra. The magnitude of the measurement range and its linearity were the

evaluation parameter. For the experimental verification of the performance measurement, a variant of a pair of gratings for the measurement of small deformations was selected, in Table 1 marked as #2. The above-stated Bragg gratings have a spectral width of 1 mm, they are spectrally spaced by 0.5 nm from each other and exhibit reflectivity of 95%. With respect to the production tolerances of Bragg gratings, gratings in polyimide protection with the parameters listed in Table 3 were produced. The spectral shift between the gratings is 465 pm.

Table 3. The parameters of the pair of Bragg gratings used for experimental verification of the passive detection scheme design

Parameter	FBG_R (nm)	FBG_M (nm)
Bragg wavelength	1549.7	1550.165
Spectral width	1.019	1.012
Reflectivity	92.05	92.05

The chain of two Bragg gratings was verified by power measurement, as shown in Fig. 2. The light from a wide-spectrum SLED (Superluminescent Light Emitting Diode) source with a spectral width of 90 nm and a power output of 1 mW was led, via a circulator, to a pair of Bragg gratings. The reference Bragg grating was not loaded anyhow. The measured Bragg grating was clamped into a mechanical stretcher and stretched from 0 mm to 0.5 mm in steps of 0.02 mm. The distance between the extreme fixed points was 650 mm.

Fig. 10 shows the reflection spectra of the pair of Bragg gratings for selected deformations of the measurement Bragg grating. The blue curve shows the overlapping spectra of both gratings in the unloaded state. The purple curve shows the reflection spectrum for the maximum load of the measurement grating, which corresponds to 769 μstrain.

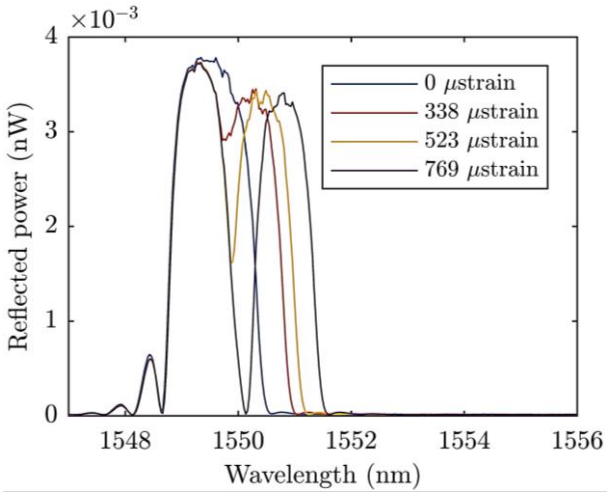

Fig. 10. The reflection spectra of the pair of Bragg gratings of the passive detection scheme for the selected deformation effects on the measurement Bragg grating

Fig. 11 shows the magnitude of power reflected from the pair of Bragg gratings, depending on the deformation effect on the Bragg grating measured in a range from 0 to 769 μstrain. The blue curve shows the dependence obtained from the simulation with configuration # 2 according to Table 1, the red curve shows experimental results from the measurement with a pair of gratings with the parameters listed in Table 3.

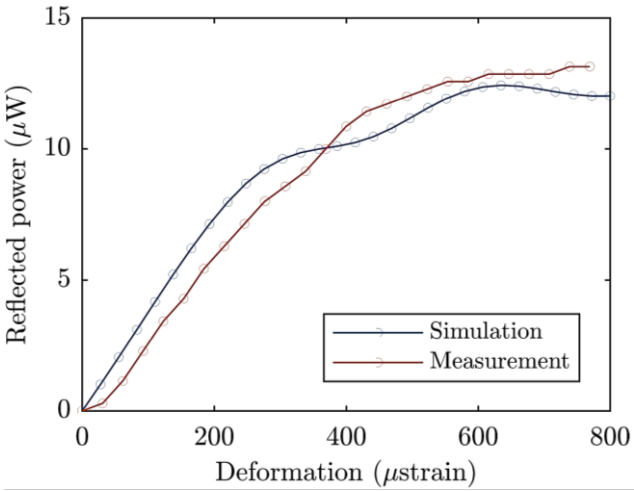

Fig. 11. The results of the power measurement with the measurement Bragg grating clamped into the mechanical tensioner

5. Conclusion

In practice, passive detection schemes were quickly replaced with spectral analysers that can evaluate tens of sensors at the same time. The big problem, however, is the high purchase price of the spectrum analyser in case of necessity of one-point measurement. The simulation results show suitable configurations of the pair of Bragg gratings, their linearity and the magnitude of the measurement range The most suitable configurations indicate that the spectral distance should be from 25% to 55% of the width of the Bragg grating spectrum. A configuration with Bragg gratings with a spectral distance of 465 pm, spectrum widths of 1.019 nm and 1.012 nm and reflectivity of 92% for the measurement of deformations from 0 to 769 μstrain was then experimentally verified. Although the conversion characteristic is not linear in its entire extent, it can be connected with an approximation straight line, thus implementing precise and economical measurement in places where conventional sensor types cannot be used due to electromagnetic interference, unavailable power supply, among several others.

Acknowledgments

This work was supported by the VŠB-TUO Student grant projects. The project registration number is

SP2018/55. This work was also supported by the European Regional Development Fund in the Research Centre of Advanced Mechatronic Systems project, project number CZ.02.1.01/0.0/0.0/16_019/0000867 within the Operational Programme Research, Development and Education.

References

[1] S. Melle, K. Liu, R. Measures, IEEE Photonics Technology Letters **4**(5), 516 (1992).
[2] A. Ribeiro, L. Ferreira, M. Tsvetkov, J. Santos, Electron. Lett. **32**(4), 382 (1996).
[3] R. Fallon, L. Zhang, A. Gloang, I. Benion, Electron. Lett. **33**, 705 (1997).
[4] M. Davis, A. Kersey, Electron. Lett. **30**(1), 75 (1994).
[5] S. Melle, K. Liu, R. M. Measures, IEEE Photonics Technol. Lett. **4**(5), 516 (1992).
[6] J. Peupelmannm, J. Meissner, Proc. 13th Int. Conf. Optical Fiber Sensors (OFS-13), Kyongju, Korea, Proc. SPIE **3746**, 470 (1999).
[7] R. Fallon, L. Zhang, A. Gloang, I. Bennion, Electron. Lett. **33**(8), 705 (1997).
[8] L. Zhang, R. W. Fallon, A. Gloang, I. Bennion, F. M. Haran, P. Foote, Proc. Optical Fiber Sensors Conference (OFS-12), 452 (1997).
[9] M. A. Davis, A. D. Kersey, Proc. Optical Fiber Sensors Conf. (OFS-10), Glasgow, Scotland 167 (1994).
[10] D. A. Flavin, R. Mcbride, J. D. C. Jones, Electron. Lett. **33**(4), 319 (1997).
[11] M. Volanthen, H. Geiger, M. G. Xu, J. P. Dakin, Electron. Lett. **32**, 1228 (1996).
[12] M. G. Xu, H. Geiger, J. L. Archambault, L. Reekie, J. P. Dakin, Electron. Lett. **29**, 1510 (1993).
[13] M. G. Xu, H. Geiger, J. P. Dakin, J. Lightwave Technol. **14**, 391 (1996).
[14] K. O. Hill, Y. Fujii, D. C. Johnson, B. S. Kawasaki, Appl. Phys. Lett. **32**(10), 647 (1978).
[15] T. Erdogan, J. Lightwave Technol. **15**(8), 1277 (1997).
[16] A. D. Kersex, M. A. Davis, H. J. Patrick, M. Leblanc, K. P. Koo, C. G. Askins, M. A. Putnam, E. J. Friebele, J. Lightwave Technol. **15**(8), 1442 (1997).
[17] M. Fajkus et al., Adv. Electr. Electron. Eng. **13**(5), 575 (2015).
[18] M. Fajkus et al., Sensors **17**(1), 111 (2017).
[19] W. Zhang et al., Optics Express **27**(2), 461 (2019).

*Corresponding author: marcel.fajkus@vsb.cz